Society For Biomaterials

The effect of four types of artificial nerve graft structures on the repair of 10-mm rat sciatic nerve gap

Chan Zhou,[1] Bin Liu,[2] Yong Huang,[1] Xiu Zeng,[1] Huajian You,[2,3] Jin Li,[1,2] Yaoguang Zhang[2]

[1]Chongqing Academy of Animal Science, Chongqing 400015, China
[2]Key Laboratory of Freshwater Fish Reproduction and Development, Ministry of Education, School of Life Sciences, Southwest University, Chongqing 400715, China
[3]Chongqing academy of Chinese medicine, Chongqing 400065, China

Received 8 June 2017; revised 1 July 2017; accepted 1 August 2017
Published online 21 August 2017 in Wiley Online Library (wileyonlinelibrary.com). DOI: 10.1002/jbm.a.36172

Abstract: Investigating the effect of four types of artificial nerve graft (ANG) structures on rat sciatic nerve defect repair will aid future ANG designs. In this study, fibroin fibers and polylactic acid were used to prepare four ANGs with differing structures: nerve conduit with micron-sized pores (Conduit with pore group), nerve conduit without micron-sized pores (Conduit group), nerve scaffold comprising Conduit with pore group material plus silk fibers (Scaffold with pore group), and nerve scaffold comprising Conduit group material plus silk fibers (Scaffold group). ANGs or autologous nerves (Autologous group) were implanted into 10 mm rat sciatic nerve defects (n = 50 per group). Twenty weeks after nerve grafting, the time required to retract the surgical limb from the hot water was ranked as follows: Conduit with pore group > Scaffold with pore group > Conduit group > Scaffold group > Autologous group. The static sciatic index was ranked in descending order: Autologous group > Scaffold group > Conduit group > Scaffold with pore group > Conduit with pore group. Immunofluorescence staining identified significant differences in the distribution and number of axons, Schwann cells, and fibroblasts. These findings indicate that ANGs with micron-sized pores had a negative impact on the repair of peripheral nerve defects, while internal microchannels were beneficial. © 2017 The Authors. Journal of Biomedical Materials Research Part A Published by Wiley Periodicals, Inc. J Biomed Mater Res Part A: 105A: 3077–3085, 2017.

Key Words: artificial nerve, fibroin fiber, conduit, scaffold, rat sciatic nerve defect

How to cite this article: Zhou C, Liu B, Huang Y, Zeng X, You H, Li J, Zhang Y. 2017. The effect of four types of artificial nerve graft structures on the repair of 10-mm rat sciatic nerve gap. J Biomed Mater Res Part A 2017:105A:3077–3085.

INTRODUCTION

The incidence of peripheral nerve defects is high, and with a lack of suitable nerve replacement grafts, repair rates remain low.[1,2] Development of artificial nerve grafts (ANGs) to replace autologous nerve grafts is under intense research.[3–12] A neural conduit is an ANG with a hollow tubular structure,[13–19] while a conduit with filler is referred to as a nerve scaffold.[20,21] There is a popular belief that the presence of micron-sized pores on the neural conduit wall favors the exchange of materials between the internal and external environment of the neural conduit, which is beneficial for nerve regeneration. Therefore, porosity is considered to be an important indicator for the assessment of neural conduits.[22] Given the existing evidence that the presence of pores on the nerve conduit wall can impede nerve regeneration,[23] we try to explore whether the presence of micron-sized pores on the wall of neural conduit prepared in this study affects peripheral nerve repair negatively or positively.

The presence or absence of pores on the neural conduit wall is a relative concept; indeed, the presence of nanometre-sized pores is inevitable because of the naturally produced honeycomb structures during solvent volatilization during the preparation of the neural conduit.[24] However, micron-sized pores can be eliminated or added through artificial interventions. Existing pores on the wall of a neural conduit made of hydrogel are generally produced following hydrogel drying. Interestingly, these pores change in response to the tissue fluid when implanted *in vivo*. Consequently, the morphology of micron-sized pores fabricated with insoluble material in this study cannot change by the tissue fluid after implanted into animals.

Previous studies have shown that the internal structures of ANGs directly influence their restorative effects on peripheral nerve defects.[7] Based on this, microchannels inside artificial nerves have been developed, with representative numbers such as, 2, 4, and 7[25]; 8[26]; 9[27]; 30[22]; 59, 84, and 143.[11] Given that the diameter of peripheral nerves is relatively fixed, higher numbers of microchannels result in smaller microchannel diameters. Many artificial fibers are reported to be filled with a neural conduit to generate a

Correspondence to: Y. Huang; e-mail: yonghuangcq@163.com or B. Liu; e-mail: xytom@swu.edu.cn
Contract grant sponsor: Fund of Chongqing Agricultural Development; contract grant number: 16403
Contract grant sponsor: National Natural Science Foundation of China; contract grant number: 31271036

nerve scaffold.[3] In studies of peripheral nerve repair using artificial nerve constructions, the neural conduit[28,29] is typically a millimeter-sized single channel, while inside the nerve scaffold[5,7] there exist micron-sized[25,27] or nanometre-sized[3] microchannels. Whether these microchannels are interconnected or in parallel may affect the extending direction of the axon. A single axon is micron-sized and cannot pass through a nanometre-sized microchannel. To date, it remains unclear whether it is the microchannels or the materials themselves that are responsible for guiding regeneration of the nerve fibers. Therefore, the materials we used here to make these microchannels were considered as a track to guide axonal regeneration. Statistically, the number of nerve fibers on the cross section of the rat sciatic nerve is about 6000× This said, it is rational to ensure that the artificial nerve is equipped with a similar amount of microchannels or tracks. Therefore, we placed ~6000 fibroin fibers into the nerve conduit, and the adjacent gaps between these fibers were considered as microchannels or tracks to guide axonal regeneration. Peripheral nerve fibers are composed of axons and Schwann cells, and fibroblasts are involved in the early repair of peripheral nerve defects.[30] New cell types and tissues in the graft are directly related to the repair effect. Therefore, in our study, cell types in the newly formed tissues inside the artificial nerves served as an indicator to evaluate peripheral nerve defect repair.

Natural silk fiber is composed of fibroin and sericin; and after removal of sericin, the silk fiber becomes water insoluble fibroin fiber.[31–33] Water-soluble regenerated fibroin is representative of the silk used in tissue engineering,[34] such as in artificial neural research.[13,24,28,31] However, the application of natural fibroin fibers has not yet been reported in artificial neural research.

We prepared four structurally different ANGs: (1) a nerve conduit with micron-sized pores on its wall (Conduit with pore group), (2) a nerve conduit without micron-sized pores on its wall (Conduit group), (3) a nerve scaffold composed of Conduit with pore group material with fibroin fiber microchannels or tracks (Scaffold with pore group), and 4) a nerve scaffold composed of Conduit group material with fibroin fiber microchannels (Scaffold group). To evaluate their effects, with or without pores and internal microchannels, in peripheral nerve repair, autologous nerve grafting was used as a control (Autologous group), meanwhile artificial and autologous nerve grafts were implanted into a 10 mm sciatic nerve defect in rats. Sensory and motor functional recoveries of surgical limbs were assessed according to previously reported methods.[35,36] Cell types in the grafts were determined using immunofluorescence staining. These measurements provided evidence for studying the morphology and structure of the artificial nerves.

MATERIALS AND METHODS

Preparation of ANGs

Silk fabric (175 mesh, plain weaving) was provided by Bio-Technology College of Southwest University, China. During the silk fabric weaving process, square pores of about 20 μm in width formed naturally on its surface. The silk fabric was cut to strips (12 × 12 mm), and immersed in a 0.5% (W/V)$NaCO_3$ aqueous solution. The solution was stirred at 100°C for 1 h using a constant magnetic stirrer (type 85–2, Shanghai Instrument Co., Shanghai, China), then placed in deionized water and stirred at 70°C for 1 h. The experimental procedures were repeated three times, and the silk fabric strips were removed and dried using ventilation equipment (CS101–2 A BN, Chongqing Immortalized ExperimentalInstrument Factory, China) at 40°C.

To prepare a semi-finished tube, silk fabric strips were immersed for 2 h in a chloroform solution containing 10% (W/V) polylactic acid (PLA; molecular weight 200,000 Daltons; Esun, Shenzhen, China), removed from the solution and wound tightly twice around a stick (with an outer diameter of 1.8 mm.), then covered with a fixing strip (12 × 100 mm), and dried using ventilation equipment. Next, the stick and fixing strip were removed.

To prepare the tube, along the longitudinal axis of the semi-finished tube, over-and-over whip sutures were applied with a needle to fix the cross- sections of the silk fabric strip that formed the semi-finished tube, and another 3 suture lines were applied along the longitudinal axis of the semi-finished tube, evenly distributed along the circumference of the tube, to tie the two layers of silk fabric strips.

These tubes were used to prepare two types of nerve conduits. For both conduit types, tubes were immersed for 2 h in the chloroform solution and dried naturally at room temperature. For the first type, the conduit was re-immersed in PLA solution for 1 min and air-dried: this process was repeated several times in order for the original wall pores to become blocked by PLA [Conduit; Fig. 1(E)]. The second nerve conduit type presented with the original wall pores and it was simply covered with PLA [Conduit with pore; Fig. 1(C)]. To generate the two nerve scaffolds, 6000 fibroin fibere longer than 20 mm were prepared as a bundle, and drawn inside the tubes (both nerve conduit types) with a string. Subsequently, the tubes with the 6000 fibroin fibers inside were cut to a length of 12 mm, resulting in the generation of one with microchannels and micron-sized pores [Scaffold with pore; Fig. 1(D)] and another with microchannels, but not micron-sized pores [Scaffold; Fig. 1(F)].

Artificial nerve grafting

Sprague-Dawley rats, weighing 250 ± 10 g, were provided by the Experimental Animal Center of the Third Military Medical University affiliated to the People's Liberation Army, China. One hind limb on each rat was randomly selected for artificial nerve grafting. Preparation of the 10 mm sciatic nerve defect animal model and nerve grafting surgical implantation were carried out in accordance with a previously described method.[5] In brief, the nerve graft (Autologous, Conduit, Conduit with pore, Scaffold, or Scaffold with pore; $n = 50$/group) was implanted to bridge the 10 mm sciatic nerve defect.

Sensory function testing

In accordance with previous studies,[35] all rats were fixated at 1–17 and 20 weeks post-surgery, to ensure the surgical

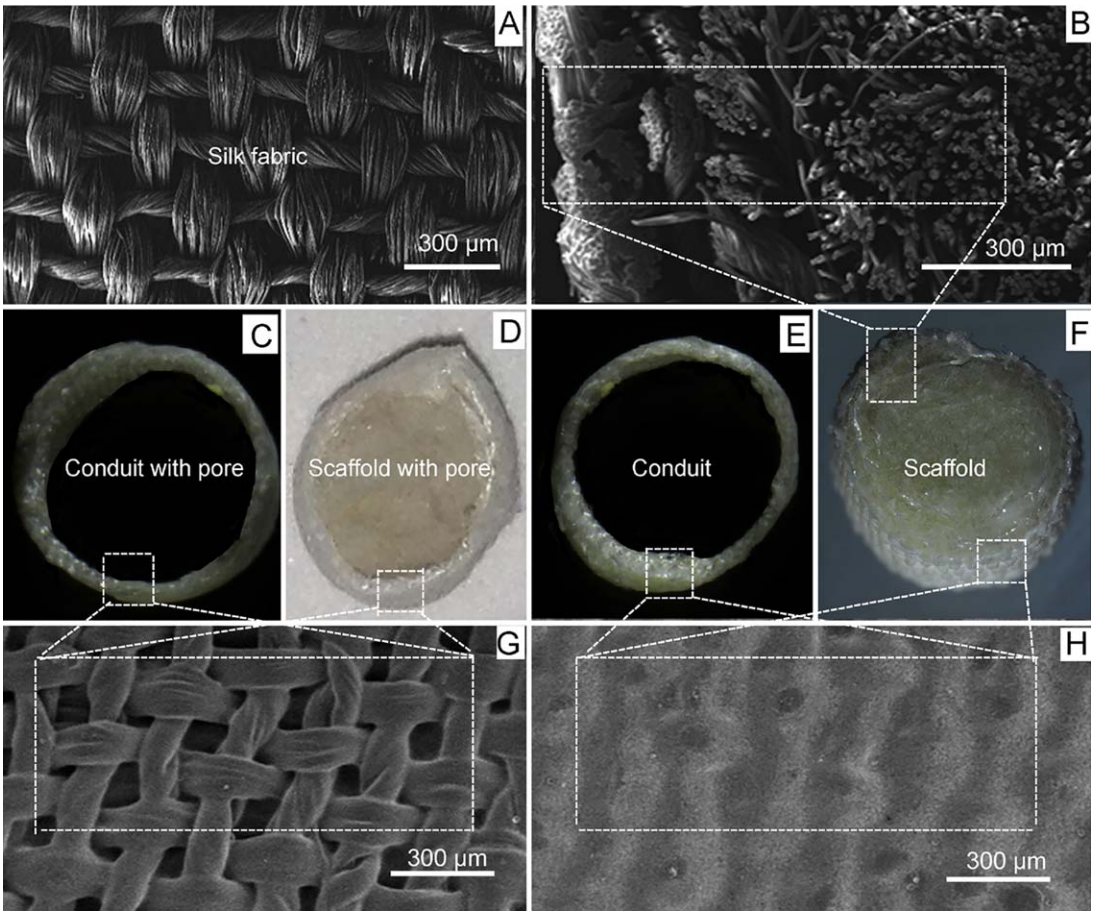

FIGURE 1. Structure of the nerve grafts. A: Silk fabric (SEM), B: Nerve scaffold with an inner structure of microchannels and a wall without micron-sized pores (SEM), C: Shape of nerve conduit with micron-sized pores, D: Shape of nerve scaffold with an inner structure of microchannels and a wall with micron-sized pores, E: Shape of nerve conduit without micron-sized pores, F: Shape of nerve scaffold with an inner structure of microchannels and a wall without micron-sized pores, G: Nerve conduit surface with micron-sized pores (SEM), H: Nerve conduit surface without micron-sized pores (SEM).

limb was immersed in a hot water bath at a constant temperature of 50°C. The time required to retract the limb in response to this heat stimulus was recorded to assess the recovery of the sensory function in the operated rats. The time of Sham Operation limb retraction was also recorded and calculated as an average from the data obtained from all experimental rats: the mean value was considered as the control.

Motor function testing

In accordance with literature,[36] the static sciatic index (SSI) was measured in rats at 1–20 weeks after surgery.

Morphological and immunofluorescent observation of the nerve grafts

At specified time points after nerve grafting, the artificial nerve bridging effects were evaluated by observing the graft appearance. Grafts were frozen (–80°C), sectioned (6 μm thickness) using a cryostat (CM1850, LEICA, Germany), stained using immunofluorescent markers, and examined under a laser scanning confocal microscope (LSM200, Zeiss, Germany) to identify different cell types within the graft. Nuclei were stained blue using 4′,6-diamidino-2-phenylindole (Biosynthesis Biotechnology, China). Primary antibody for low-affinity nerve growth factor receptor (NGFR) P75 (goat anti-rat; Santa Cruz Biotechnology, USA) was used to identify Schwann cells. Primary antibodies against fibronectin (goat anti-rat; Santa Cruz Biotechnology) and NF200 (rabbit anti-rat; Sigma, USA) were used to identify fibroblasts and axons, respectively. Schwann cells and fibroblasts were labeled green using donkey anti-goat secondary antibody and axons were marked red using donkey anti-rabbit secondary antibody (Life Technologies, USA). Specific steps for immunofluorescence staining were performed according to the manufacturer's instructions.

Statistical analysis

All data of motor and sensory function test were statistically analyzed using SPSS software, to compared their differences among the different time points in the same group or among groups at the same time point, and illustrated using Origin 8.0 software.

All data were regression analyzed to distinguish the effect of pores and microchannels on nerve defect repair as shown below.

We assumed a regression model:

$$y_i=\alpha+\beta_1X_1+\beta_2X_2+\mu_i \quad (1)$$

y_i= value (mean) of experimental group – value (mean) of Autologous group

α is a constant, X_1 and X_2 are dummy variables.

$$X_1=\begin{cases}1, & \text{ANG with micron-sized pores}\\ 0, & \text{ANG without micron-sized pores}\end{cases} \quad (2)$$

$$X_2=\begin{cases}1, & \text{ANG with microchannels}\\ 0, & \text{ANG without microchannels}\end{cases} \quad (3)$$

β_1 and β_2 respectively are dummy variable regression coefficients of X_1 and X_2.

μ is a stochastic error term.

$$\mu\sim N(0,\sigma^2) \quad (4)$$

Rewriting formula (1) as:

$$\hat{y}_i=\hat{\alpha}+\hat{\beta}_1X_1+\hat{\beta}_2X_2 \quad (5)$$

$\hat{\beta}_1$ and $\hat{\beta}_2$, respectively, are estimators of β_1 and β_2. By formulas (1) and (5), residual error e_i can be obtained as:

$$e_i=y_i-\hat{y}_i \quad (6)$$

By ordinary least square, the best way to estimate a regression model is to choose values of $\hat{\beta}_1$ and $\hat{\beta}_2$ (estimators of β_1 and β_2) to let residual error e_i to achieve minimum.

$$\min\sum e_i^2=\sum(y_i-\hat{y}_i)^2 \quad (7)$$

Regression analysis data is presented in Table I.

Stata 10 software was used to calculate formula (7) to obtain the estimator of β_1 and β_2.

If $\beta_1>0$, then it indicates that the pores will increase the value of y_i; otherwise, the pores will reduce the value of y_i. If $\beta_2>0$, then it indicates that the microchannels will increase the value of y_i; otherwise, the microchannels will reduce the value of y_i.

TABLE I. A Sample Table of Regression Analysis Data Arrangement

Y_i	X_1 (pore)	X_2 (microchannel)
Conduit group–Autologous group	0	0
Scaffold group–Autologous group	0	1
Conduit whit pore group–Autologous group	1	0
Scaffold with pore group–Autologous group	1	1

RESULTS

Results from the sensory function testing

The mean time for Sham Operation limb retraction was 0.74 s. As shown in Figure 2, within 1 week after nerve grafting, inter- or intra-group comparison measured a non-significant difference in surgical limb retraction time of ~2.63 s. At 1–8 weeks after nerve grafting, data indicated irregularity. At 4–8 weeks after nerve grafting, no significant differences in surgical limb retraction times were observed between Conduit with pore and Conduit groups, but both were longer compared with Scaffold with pore and Scaffold groups. Taken together, these findings indicate that at 4–8 weeks after nerve grafting, a shorter time for surgical limb retraction was detected in rats that had undergone implantation of nerve scaffolds with microchannels (Scaffold, Scaffold with pore groups) compared with those that had undergone implantation of nerve conduits without microchannels (Conduit with pore, Conduit groups).

At 12–20 weeks after nerve grafting data indicated regularity, intergroup comparisons revealed significant differences for surgical limb retraction times as follows: Conduit with pore group > Scaffold with pore group > Conduit group > Scaffold group > Autologous group. As shown in Figure 2, surgical limb retraction time was significantly shorter in the Conduit and Scaffold groups without micron-size pores compared with Conduit with pore and Scaffold with pore groups with micron-sized pores. This implicates that micron-sized pores in the wall of ANGs are not conducive to bridging peripheral nerve defect. Similarly, a shorter surgical limb retraction time was observed in Scaffold with pore and Scaffold groups with microchannel structures compared with Conduit with pore and Conduit groups without microchannels (Scaffold with pore group < Conduit with

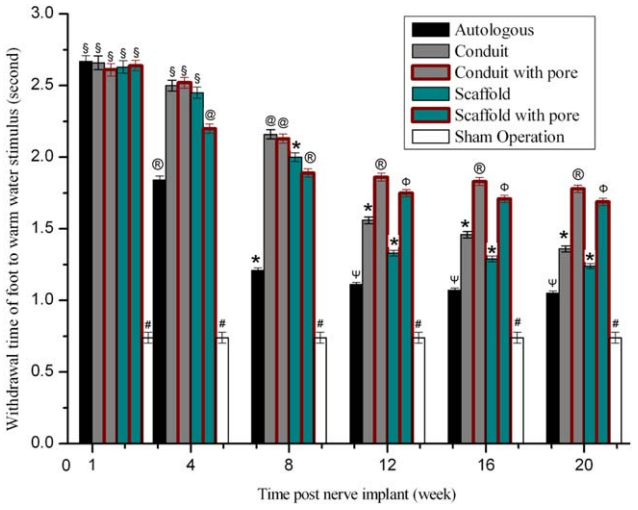

FIGURE 2. Withdrawal time of foot from the hot water. After statistical analysis ($p>0.05$), the values symboled with the same characters (§, @, ®, #, Φ, or Ψ) indicated no significant difference, while the values symboled with the different characters (§, @, ®, #, Φ, Ψ, or *) indicated significant difference. "*" Indicated the values showed significant difference.

TABLE II. Regression Analysis of Data Obtained from the Sensory Function Test (10th–20th Week)

	Coefficient	SE	t	$P>\|t\|$
β_1	0.37	0.014	27.00	0.00
β_2	−0.16	0.014	−11.45	0.00
a	0.39	0.011	32.97	0.00

TABLE III. Regression Analysis of Data Obtained From the Motor Function Test (10th–20th Week)

	Coefficient	SE	t	$P>\|t\|$
β_1	−5.75	0.72	−7.98	0.00
β_2	3.72	0.72	5.16	0.00
A	−13.08	0.62	−20.96	0.00

pore group, Scaffold group < Conduit group). This implicates that microchannels inside ANGs are conducive to bridging peripheral nerve defects. Therefore, we conclude from these findings that micron-sized pores and microchannels function negatively and positively, respectively, to bridge peripheral nerve defects.

At 10–20 weeks after nerve grafting, The results (Table II) of the regression analysis of data obtained from the sensor function test showed that $\beta_1 = 0.37 > 0$ and $\beta_2 = -0.16 < 0$. $\beta_1 > 0$ indicates that the pores increased the value of y_i. $\beta_2 < 0$ indicates that the microchannels reduced the value of y_i. In the sensor function test, longer time (y_i) corresponded to a poorer effect of ANG on nerve defect repair. Therefore, these findings indicated that pores and microchannels function negatively and positively, respectively, to bridge nerve defects.

Results from the motor function testing

As shown in Figure 3, at 1–4 weeks after nerve grafting, there were no significant differences in SSI + 100 values between groups. At 8–20 weeks after nerve grafting, with the exception of the data from published literature[36] (Fig. 3, M. B group), the Autologous group had the highest SSI + 100 value over the Scaffold group, followed by the Conduit, Scaffold with pore, and Conduit with pore groups. Furthermore, SSI + 100 values in the Scaffold and Conduit groups without micron-sized pores were higher than those in the Scaffold with pore and Conduit with pore groups

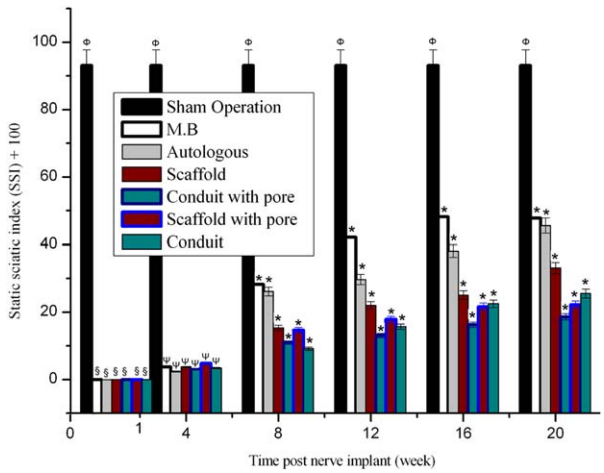

FIGURE 3. Static sciatic index. After statistical analysis ($p > 0.05$), the values symboled with the same characters (Φ, §, or Ψ) indicated no significant difference, while the values symboled with the different characters (Φ, §, Ψ, or *) indicated significant difference. "*" Indicated the values showed significant difference.

with micron-sized pores. This suggests that the presence of micron-sized pores on the wall of ANGs is not conducive to peripheral nerve repair. SSI + 100 values in the Scaffold and Scaffold with pore groups with microchannels were respectively higher than those in the Conduit and Conduit with pore groups without microchannels. This indicated that ANGs with microchannels facilitated peripheral nerve repair. As reported previously in,[36] the nerves were sutured directly following the sciatic nerve transection and the SSI + 100 values were detected at a series of time points. The SSI + 100 values of the artificial nerves in all experimental groups, the Autologous group (control) and M. B group should theoretically be in ascending order, which was in agreement with the results of this study.

At 10–20 weeks after nerve grafting, The results (Table III) of the regression analysis of data obtained from the motor function test showed that $\beta_1 = -5.75 < 0$ and $\beta_2 = 3.72 > 0$. $\beta_1 < 0$ indicates that the pores reduced the value of y_i. $\beta_2 > 0$ indicates that the microchannels increased the value of y_i. In the motor function test, higher SSI value (y_i) corresponded to a better effect of ANG on nerve defect repair. Therefore, these findings indicated that pores and microchannels function negatively and positively, respectively, to bridge nerve defects.

Internal and external nerve graft structures

The nerve graft morphology was observed at a series of time points after nerve grafting in order to evaluate biocompatibility. As shown in Figure 4, at 4 weeks post-grafting, all four types of ANGs achieved proximal and distal fusion with the sciatic nerve in the rat recipients. There were no neoplastic tissues on the graft surface and no adhesions with adjacent muscle tissues, indicating that all ANGs had good biocompatibility. A smoother surface was observed on the Conduit [Fig. 4(C)] and Scaffold [Fig. 4(D)] graft groups without micron-sized pores compared with the Conduit with pore [Fig. 4(B)] and Scaffold with pore [Fig. 4(E,F)] graft groups with micron-sized pores, in all groups indicating incomplete degradation of PLA. Moreover, the graft walls remained sealed. When compared with pre-transplantation (Fig. 1), the gaps between fibroin fibers inside the implanted grafts [Fig. 4(E)] were full of biological tissues, and the nerve ends were bridged and healed. At 20 weeks post-grafting, it was difficult to distinguish between the grafting segment and the residual sciatic nerve in terms of texture, color, and diameter.

At 20 weeks post-grafting, fibroblasts were absent on the cross section of the Autologous group, with axons and nuclei arranged regularly [Fig. 5(A)]. More axons and fewer

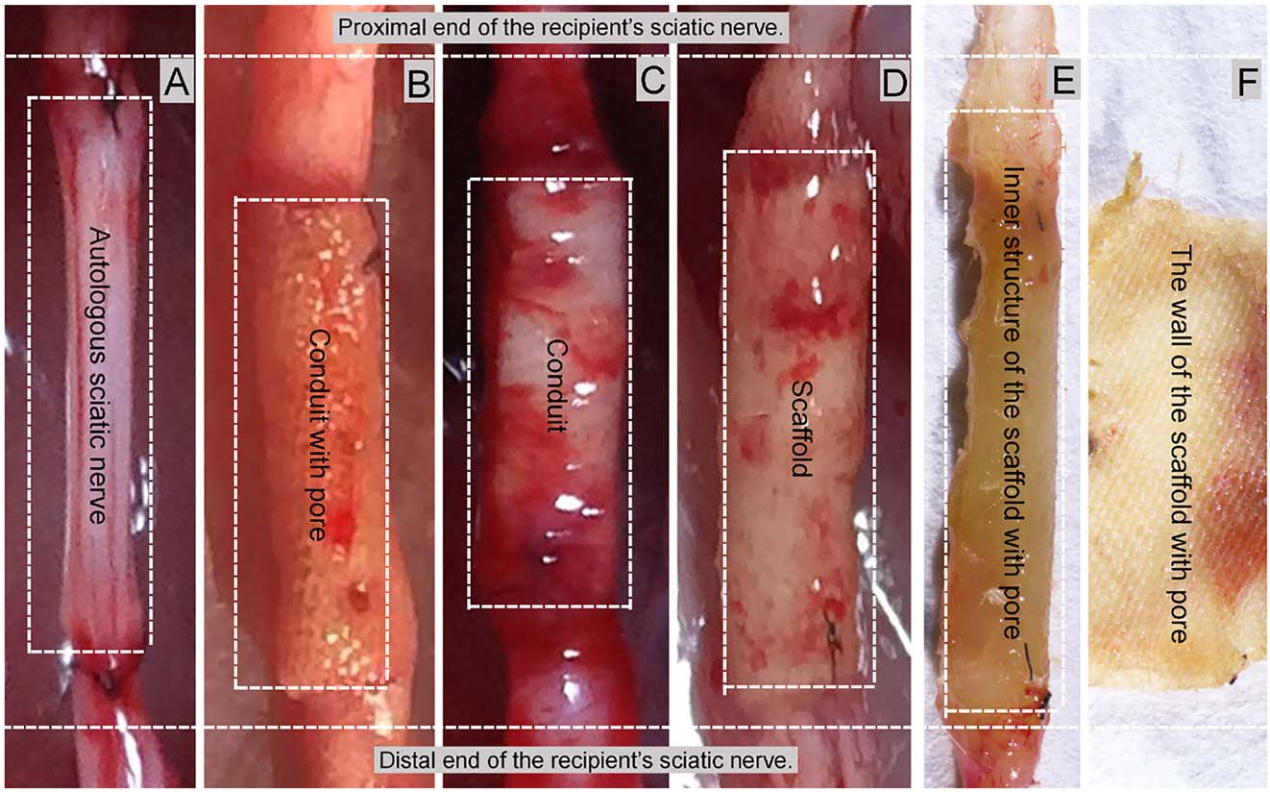

FIGURE 4. Shape of the grafts after nerve grafting. A: Autologous sciatic nerve group (0 week), B: Conduit with pore group (4 weeks), C: Conduit group (4 weeks), D: Scaffold group (4 weeks), E, F: Anatomic structure of the scaffold with pore group (4 weeks).

fibroblasts were observed in the Scaffold group [Fig. 5 (B)] compared with the Scaffold with pore group [Fig. 5 (C)]. This was also the case in the Conduit group [Fig. 4 (D)] compared with the Conduit with pore group [Fig. 4 (E)].

At 20 weeks post-grafting, a large number of Schwann cells, axons, and nuclei were present on the cross section of the Autologous group [Fig. 6(A)]. A greater number of axons and Schwann cells were observed in the Scaffold group [Fig. 6(B)] compared with the Scaffold with pore group [Fig. 6(C)], and similarly in the Conduit group [Fig. 6(D)] compared with the Conduit with pore group [Fig. 6(E)]. In the Conduit with pore group, axons were distributed noticeably unevenly as clusters.

DISCUSSION

The rat sciatic nerve contains both afferent and efferent nerve fibers. Therefore, the degree of sensorimotor functional recovery indirectly reflects the repair effect of ANGs on sciatic nerve defects.[35,36] Nerve conduction is achieved via the axon, while Schwann cells form a myelin sheath wrapping around the axon. Thus, the number of axons and Schwann cells on the cross section of a nerve graft intuitively reflects the merits and demerits of tissue repair. Fibroblasts were clearly absent in the cross section of the normal sciatic nerve. The higher number of fibroblasts in the cross section of the nerve grafts indicate inferior sciatic nerve repair.

With respect to tissue inflammation, an inflammatory response is elicited following grafting. Grafts with poor biocompatibility will be regarded as foreign intruders by the body, resulting in the formation of a connective tissue capsule (neoplasm) on the graft surface, thus isolating the graft from normal tissues. In our study, none of the four ANGs resulted in neoplastic tissue formation on their surfaces and no adhesions with adjacent muscle tissues were observed. This indicates that all the ANGs had good biocompatibility.

With respect to the effects of ANGs with pores on rat sciatic nerve 10 mm defect repair, both our sensory and motor function tests suggested that the presence of micron-sized pores on the outer wall of ANGs prepared in this study is not favourable to the afferent nerve fiber repair. In fact, the micron-sized pores were shown to inhibit axonal regeneration and facilitate fibroblast infiltration and growth. Furthermore, the micron-sized pores did not promote axonal regeneration and Schwann cell proliferation. These findings suggest that ANGs with micron-sized pores on their walls is not better to the peripheral nerve repair than those without micron-sized pores.

Material exchange is necessary during the repair of peripheral nerve defects. In the normal sciatic nerve, material exchange may be achieved as follows: (1) via the capillaries inside the nerve; (2) through the flow of cytoplasm within the axon; and (3) between adjacent cells and the extracellular matrix. After nerve grafting, the gap between the nerve ends is filled with tissue fluid that is responsible

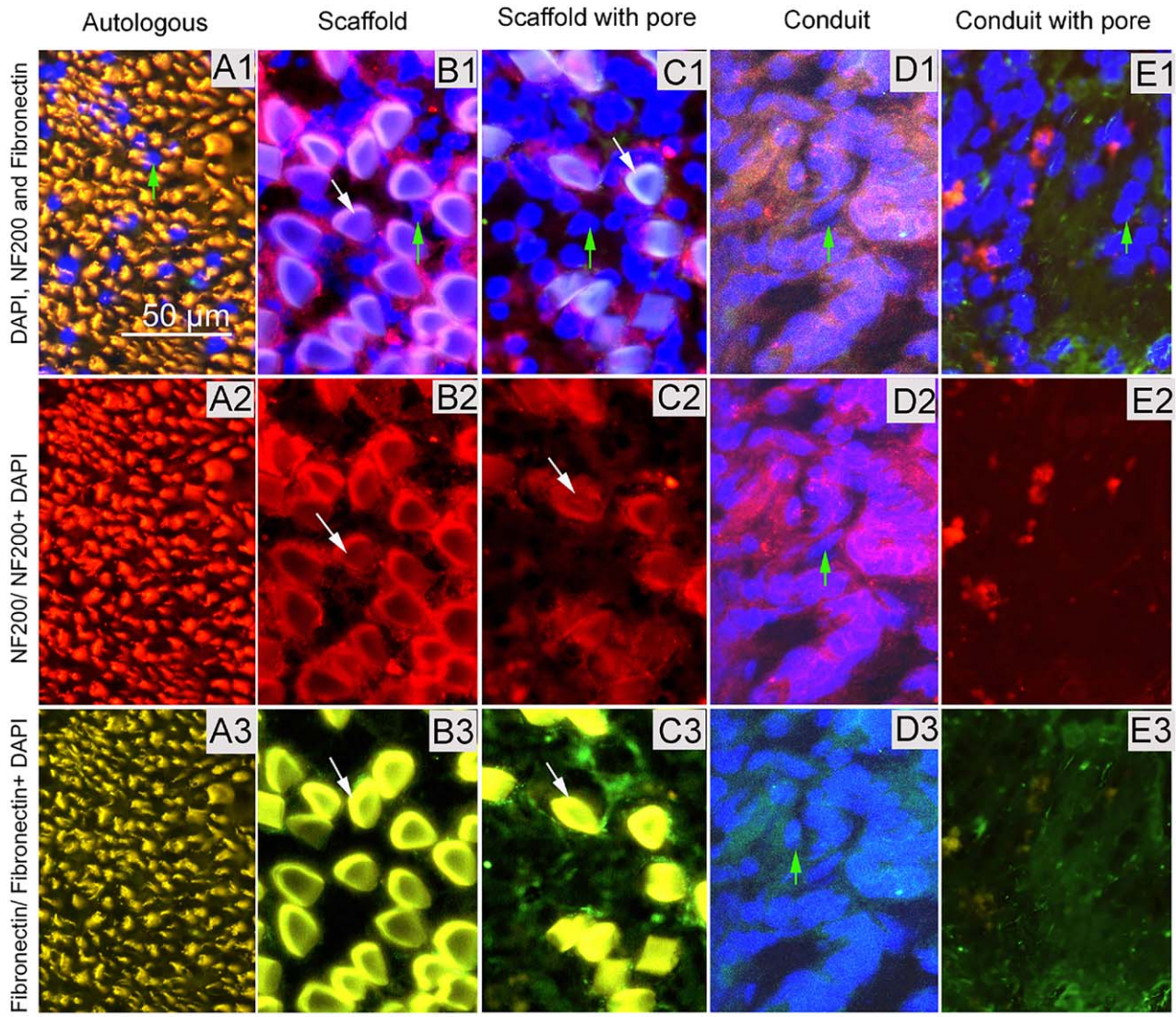

FIGURE 5. Immunofluorescence of nerve graft frozen sections stained with DAPI (blue), NF200 (red), and Fibronectin (green) at 20 weeks after implantation. A: Autologous group, B: Scaffold group, C: Scaffold with pore group, D: Conduit group, E: Conduit with pore group. White arrow: Fibroin fiber. Green arrows: nuclei.

for substance exchange in the ANG. Material exchange can therefore occur in ANGs with no pores for nerve regeneration. In general, cells and tissues adjacent to an ANG, such as inflammatory cells, have the opportunity to enter into micron-sized pores (>5 μm in diameter) and successively proliferate.[23] We propose that the growth and proliferation of these cells interfere with the normal activity of the cells inside the ANG.

Our experimental findings suggest that the presence of microchannels inside the ANG enhances nerve fiber restoration. A highly uneven distribution of axons arranged in clusters was observed in the Conduit with pore group, indicating that the absence of microchannels is not beneficial to the required ordered arrangement of axons for peripheral nerve repair.

Representing the internal microenvironment of ANGs, microchannels greatly influence cell behaviour during nerve fibers reconstruction.[7] Studies have shown that during peripheral nerve repair, fibroblasts initially guide ordered arrangement of Schwann cells, and subsequently Schwann cells guide axonal regeneration.[30] Given that both fibroblasts and Schwann cells are adherent cells, they are both speculated to adhere preferentially to the inner wall of the ANG during repair, rather than to free-float in the lumen of the microchannels. Therefore, the mechanisms underlying the guided nerve regeneration facilitated by these microchannels may be associated with the role of microchannel materials as a track for cell growth and arrangement, to guide axonal growth. In this study, the fibroin fibers used to fill the nerve scaffolds likely acted as tracks, guiding cell growth and thereby axonal regeneration. It can be presumed that the generation of numerous parallel, with a degradation rate matching that of native peripheral nerve regeneration would benefit nerve fiber reconstruction by ANGs. In fact, a

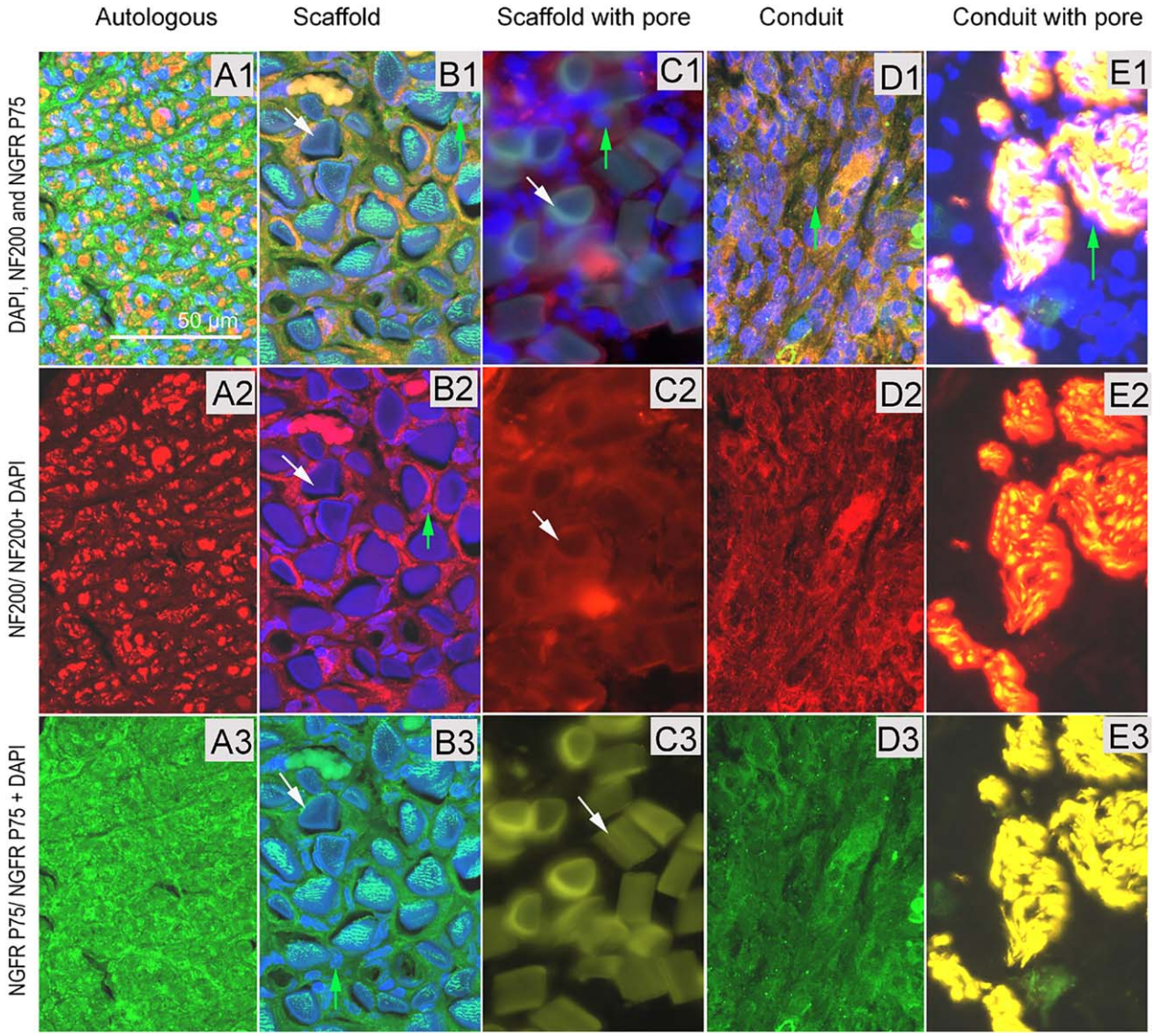

FIGURE 6. Immunofluorescence of nerve graft frozen sections stained with DAPI (blue), NF200 (red), and NGFR P75 (green) at 20 weeks after implantation. A: Autologous group, B: Scaffold group, C: Scaffold with pore group, D: Conduit group, E: Conduit with pore group. White arrow: Fibroin fiber. Green arrows: nuclei.

series of follow-up experiments is required to explore whether the presence of micron-sized pores on the neural conduit affects peripheral nerve repair negatively or positively.

CONCLUSIONS

All four types of ANGs prepared in this study had good biocompatibility, which contributed to the successful repair of peripheral nerve defects in rats. The presence of microchannels (tracks) inside the ANG favored axon regeneration and the orderly arrangement of tissues for enhanced peripheral nerve repair. It is possible that the presence of micron-sized pores on the wall of the ANG promoted fibroblast growth and inhibited Schwann cell and axonal growth, resulting in inferior peripheral nerve repair. But a series of follow-up experiments is required to explore whether the presence of micron-sized pores on the neural conduit affects peripheral nerve repair negatively or positively.

REFERENCES

1. Pateman CJ, Harding AJ, Glen A, Taylor CS, Christmas CR, Robinson PP, Rimmer S, Boissonade FM, Claeyssens F, Haycock JW. Nerve guides manufactured from photocurable polymers to aid peripheral nerve repair. Biomaterials 2015;49:77–89.
2. Ribeiro J, Caseiro AR, Pereira T, Armada-da-Silva PA, Pires I, Prada J, Amorim I, Leal Reis I, Amado S, Santos JD, Bompasso S, Raimondo S, Varejão AS, Geuna S, Luís AL, Maurício AC. Evaluation of PVA biodegradable electric conductive membranes for nerve regeneration in axonotmesis injuries - the rat sciatic nerve animal model. J Biomed Mater Res A 2017; 105:1267–1280.
3. Li A, Hokugo A, Yalom A, Berns EJ, Stephanopoulos N, Mcclendon MT, Segovia LA, Spigelman I, Stupp SI, Jarrahy R. A bioengineered peripheral nerve construct using aligned peptide amphiphile nanofibers. Biomaterials 2014;35:8780–8790.
4. Tajdaran K, Gordon T, Wood MD, Shoichet MS, Borschel GH. An engineered biocompatible drug delivery system enhances nerve

regeneration after delayed repair. J Biomed Mater Res A 2016; 104:367–376.
5. Bozkurt A, Boecker A, Tank J, Altinova H, Deumens R, Dabhi C, Tolba R, Weis J, Brook GA, Pallua N, van Neerven SG. Efficient bridging of 20 mm rat sciatic nerve lesions with a longitudinally micro-structured collagen scaffold. Biomaterials 2016;75:112–122.
6. Barbarisi M, Marino G, Armenia E, Vincenzo Q, Rosso F, Porcelli M, Barbarisi A. Use of polycaprolactone (PCL) as scaffolds for the regeneration of nerve tissue. J Biomed Mater Res A 2015;103: 1755–1760.
7. Cerri F, Salvatore L, Memon D, Martinelli BF, Madaghiele M, Brambilla P, Del Carro U, Taveggia C, Riva N, Trimarco A, Lopez ID, Comi G, Pluchino S, Martino G, Sannino A, Quattrini A. Peripheral nerve morphogenesis induced by scaffold micropatterning. Biomaterials 2014;35:4035–4045.
8. Wood MD, Kemp SWP, Liu EH, Szynkaruk M, Gordon T, Borschel GH. Rat-derived processed nerve allografts support more axon regeneration in rat than human-derived processed nerve xenografts. J Biomed Mater Res A 2014;102:1085–1091.
9. Guicai L, Luzhong Z, Yumin Y. Tailoring of chitosan scaffolds with heparin and γ-aminopropyltriethoxysilane for promoting peripheral nerve regeneration. Colloids Surf B Biointerf 2015;134:413–422.
10. Neal RA, Tholpady SS, Foley PL, Swami N, Ogle RC, Botchwey EA. Alignment and composition of laminin-polycaprolactone nanofiber blends enhance peripheral nerve regeneration. J Biomed Mater Res A 2012;100:406–423.
11. Srinivasan A, Tahilramani M, Bentley JT, Gore RK, Millard DC, Mukhatyar VJ, Joseph A, Haque AS, Stanley GB, English AW, Bellamkonda RV. Microchannel-based regenerative scaffold for chronic peripheral nerve interfacing in amputees. Biomaterials 2015;41:151–165.
12. Magnaghi V, Conte V, Procacci P, Pivato G, Cortese P, Cavalli E, Pajardi G, Ranucci E, Fenili F, Manfredi A, Ferruti P. Biological performance of a novel biodegradable polyamidoamine hydrogel as guide for peripheral nerve regeneration. J Biomed Mater Res A 2011; 98A:19–30.
13. Ghaznavi AM, Kokai LE, Lovett ML, Kaplan DL, Marra KG. Silk fibroin conduits: a cellular and functional assessment of peripheral nerve repair. Ann Plastic Surg 2011;66:273–279.
14. Goncalves C, Ribeiro J, Pereira T, Luis AL, Mauricio AC, Santos JD, Lopes MA. Preparation and characterization of electrical conductive PVA based materials for peripheral nerve tube-guides. J Biomed Mater Res A 2016;104:1981–1987.
15. Lee YS, Griffin J, Masand SN, Shreiber DI, Uhrich KE. Salicylic acid-based poly(anhydride-ester) nerve guidance conduits: impact of localized drug release on nerve regeneration. J Biomed Mater Res A 2016; 104:975–982.
16. Neubrech F, Heider S, Harhaus L, Bickert B, Kneser U, Kremer T. Chitosan nerve tube for primary repair of traumatic sensory nerve lesions of the hand without a gap: study protocol for a randomized controlled trial. Trials 2016;17:48.
17. Arslantunali D, Budak G, Hasirci V. Multiwalled CNT-pHEMA composite conduit for peripheral nerve repair. J Biomed Mater Res A 2014;102:828–841.
18. Panseri S, Cunha C, Lowery J, Del CU, Taraballi F, Amadio S, Vescovi A, Gelain F. Electrospun micro- and nanofiber tubes for functional nervous regeneration in sciatic nerve transections. Bmc Biotechnol 2008;8:39.
19. Sun M, Kingham PJ, Reid AJ, Armstrong SJ, Terenghi G, Downes S. In vitro and in vivo testing of novel ultrathin PCL and PCL/PLA blend films as peripheral nerve conduit. J Biomed Mater Res A 2010; 93:1470–1481.
20. de Boer R, Borntraeger A, Knight AM, Hebert-Blouin MN, Spinner RJ, Malessy MJA, Yaszemski MJ, Windebank AJ. Short- and long-term peripheral nerve regeneration using a poly-lactic-co-glycolic-acid scaffold containing nerve growth factor and glial cell line-derived neurotrophic factor releasing microspheres. J Biomed Mater Res A 2012;100A:2139–2146.
21. Tse KH, Sun MZ, Mantovani C, Terenghi G, Downes S, Kingham PJ. In vitro evaluation of polyester-based scaffolds seeded with adipose derived stem cells for peripheral nerve regeneration. J Biomed Mater Res A 2010; 95A:701–708.
22. Jeffries EM, Wang Y. Biomimetic micropatterned multi-channel nerve guides by templated electrospinning. Biotechnol Bioeng 2012;109:1571–1582.
23. Meek MF, Den Dunnen WF. Porosity of the wall of a neurolac nerve conduit hampers nerve regeneration. Microsurgery 2009;29: 473–478.
24. Bai S, Zhang W, Lu Q, Ma Q, Kaplan DL, Zhu H. Silk nanofiber hydrogels with tunable modulus to regulate nerve stem cell fate. J Mater Chem B Mater Biol Med 2014; 2:6590–6600.
25. Yao L, Ruiter GCWD, Wang H, Knight AM, Spinner RJ, Yaszemski MJ, Windebank AJ, Pandit A. Controlling dispersion of axonal regeneration using a multichannel collagen nerve conduit. Biomaterials 2010;31:5789–5797.
26. Dinis TM, Elia R, Vidal G, Dermigny Q, Denoeud C, Kaplan DL, Egles C, Marin F. 3d multi-channel bi-functionalized silk electrospun conduits for peripheral nerve regeneration. J Mech Behav Biomed Mater 2015;41:43–55.
27. Wang K, Li XQ, Li XX, Pei WH, Chen HD, Dong JQ. Efficacy and reliability of long-term implantation of multi-channel microelectrode arrays in the optical nerve sheath of rabbit eyes. Vis Res 2011;51:1897–1906.
28. Das S, Sharma M, Saharia D, Sarma KK, Sarma MG, Borthakur BB, Bora U. Data in support of in vivo studies of silk based gold nano-composite conduits for functional peripheral nerve regeneration. Biomaterials 2015;4:315–321.
29. Meyer C, Stenberg L, Gonzalezperez F, Wrobel S, Ronchi G, Udina E, Suganuma S, Geuna S, Navarro X, Dahlin LB, Grothe C, Haastert-Talini K. Chitosan-film enhanced chitosan nerve guides for long-distance regeneration of peripheral nerves. Biomaterials 2016;76:33–51.
30. Parrinello S, Napoli I, Ribeiro S, Wingfield DP, Fedorova M, Parkinson DB, Doddrell RD, Nakayama M, Adams RH, Lloyd AC. Ephb signaling directs peripheral nerve regeneration through sox2-dependent schwann cell sorting. Cell 2010;143:145–155.
31. Liu B, Song YW, Jin L, Wang ZJ, Pu DY, Lin SQ, Zhou C, You HJ, Ma Y, Li JM, Yang L, Sung KL, Zhang YG. Silk structure and degradation. Colloids Surf B Biointerf 2015;131:122–128.
32. Elliott DF. A search for specific chemical methods for fission of peptide bonds. I. The N-acyl to O-acyl transformation in the degradation of silk fibroin. Biochem J 1952; 50:542–550.
33. Sasaki T, Noda H. Studies on silk fibroin of bombyx mori directly extracted from the silk gland: iii. n-terminal analysis and degradation in a slightly alkaline solution. J Biochem 1974;76:493.
34. Pritchard EM, Valentin T, Boison D, Kaplan DL. Incorporation of proteinase inhibitors into silk-based delivery devices for enhanced control of degradation and drug release. Biomaterials 2011;32: 909–918.
35. Young C, Miller E, Nicklous DM, Hoffman JR. Nerve growth factor and neurotrophin-3 affect functional recovery following peripheral nerve injury differently. Restor Neurol Neurosci 2001;18:167–175.
36. Bervar M. Video analysis of standing — an alternative footprint analysis to assess functional loss following injury to the rat sciatic nerve. J Neurosci Methods 2000;102:109–116.